Article:
Jiang, Haoyu, Bao, Zilong, Wang, Mingjun et al. (5 more authors) (2023) Aerial IRS-Enabled Secure Mobile Communications: Joint 3D Trajectory and Beamforming Design. IEEE wireless communications letters. 10336899. ISSN: 2162-2345

https://doi.org/10.1109/LWC.2023.3338273

Aerial IRS-Enabled Secure Mobile Communications: Joint 3D Trajectory and Beamforming Design

Haoyu Jiang, Zilong Bao, Mingjun Wang, Wei Wang, Rui Wang, *Senior Member, IEEE*, Kanapathippillai Cumanan, *Senior Member, IEEE*, Zhiguo Ding, *Fellow, IEEE*, and Octavia A. Dobre, *Fellow, IEEE*

***Abstract*—This paper investigates a novel aerial intelligent reflecting surface (IRS)-assisted secure mobile communication system. In particular, the IRS is mounted on a unmanned aerial vehicle (UAV) to help a source transmit its confidential messages to a legitimate mobile user in the presence of a mobile eavesdropper. The aerial IRS can adjust its trajectory and phase-shift to track the moving user and provide safer communication services. Furthermore, due to the mobility of the UAV, user and eavesdropper, the effect of Doppler shifts is also taken into consideration in the channel model. Under such a setup, we formulate an average secrecy rate maximization problem to jointly optimize the 3D trajectory of the UAV and the phase-shift matrix of the aerial IRS. To deal with this non-convex optimization problem, we decompose the original problem into two subproblems and propose an iterative algorithm to determine its suboptimal solution. Numerical results show that the proposed aerial IRS-assisted 3D joint design can significantly improve the secrecy rate compared to the benchmark schemes.**

***Index Terms*—Aerial intelligent reflecting surface, UAV communications, physical layer security, trajectory design.**

I. Introduction

Unmanned aerial vehicles (UAVs) are widely used in various wireless communication networks to effectively improve the system performance due to their flexible mobility, low cost and easy deployment [1], [2]. However, the open nature of UAV-to-ground wireless channels makes the information transmission vulnerable to potential eavesdropping. Hence, various physical layer security techniques have been proposed to realize UAV secure communications in the literature, e.g., [3]–[6].

Haoyu Jiang, Zilong Bao, Mingjun Wang and Wei Wang are with the School of Information Science and Technology, Nantong University, Nantong 226019, China (e-mail: 2110310055@stmail.ntu.edu.cn; 2230310010@stmail.ntu.edu.cn; 2230320006@stmail.ntu.edu.cn; wwang2011@ntu.edu.cn).

Rui Wang is with the College of Electronics and Information Engineering, Tongji University, Shanghai 201804, China (e-mail: ruiwang@tongji.edu.cn).

Kanapathippillai Cumanan is with the School of Physics, Engineering and Technology, University of York, York YO10 5DD, U.K. (e-mail: kanapathippillai.cumanan@york.ac.uk).

Zhiguo Ding is with the Department of Electrical Engineering and Computer Science, Khalifa University, Abu Dhabi 127788, UAE, and with the Department of Electrical and Electronic Engineering, The University of Manchester, Manchester M13 9PL, U.K. (e-mail: zhiguo.ding@manchester.ac.uk).

Octavia A. Dobre is with the Faculty of Engineering and Applied Science, Memorial University, St. Johns, NL A1B 3X5, Canada (e-mail: odobre@mun.ca)

This work was supported in part by the Key Research and Development Program of Jiangsu Province under Grant BE2021013-1, in part by the UK EPSRC under grant EP/X01309X/1 and EP/W034522/1, in part by the H2020-MSCA-RISE-2020 under grant 101006411, and in part by the Canada NSERC through its Discovery program. *(Corresponding author: Wei Wang)*

Unlike the conventional physical layer security schemes, the intelligent reflective surfaces (IRS)-assisted UAV secure communications have recently drawn significant attentions as IRS can improve the received signal power at legitimate terminals while suppressing the information leakage to potential eavesdroppers via efficient beamforming designs [7]. For instance, a secrecy rate maximization problem for an IRS-assisted UAV communication system was studied in [8], where a joint scheme to design the IRS phase shifts, UAV trajectory and transmit power was proposed. Such IRS-assisted secure transmission was then extended to both the downlink and uplink of an UAV-ground communication system in [9]. In [10], some encouraging work was done to effectively extend the coverage of UAV via exploiting IRS. Moreover, an IRS-assisted secure transmission scheme was also investigated in millimeter-wave enabled UAV communication networks to increase the system secrecy rate in [11].

However, the aforementioned works have only considered terrestrial IRS-assisted UAV secure communications [8]–[11], which may not be sufficient to support high-level security performance. This is because the terrestrial IRS is usually installed on the facades of buildings, which is only effective for the users residing in its front half-space. In addition, for the complex urban environment, it is generally difficult for the terrestrial IRSs to establish line-of-sight (LoS) links with the ground nodes. Thus, an aerial IRS is highly appealing to further improve the quality of secured transmission due to the omni-directional reflection and LoS links [12], [13]. In [12], the authors considered an aerial IRS-aided UAV secure communication system, where the secrecy rate was maximized by jointly designing the deployment and the phase shifts of the aerial IRS. Further, this aerial IRS-assisted UAV secure transmission was extended to a more general scenario with multiple eavesdroppers in [13]. However, the authors in [8]–[13] assumed that the eavesdroppers are at fixed locations and the UAV flies at a fixed altitude, which may not be applicable in the complex urban mobile environments. Motivated by the aforementioned facts, in this paper we study an aerial IRS-assisted secure mobile communication system, where the IRS is mounted on a UAV to help a source transmit its confidential messages to a legitimate mobile user in the presence of a mobile eavesdropper. The main contributions are summarized as follows:

1) To the best of the authors' knowledge, this is the first work to employ the aerial IRS in the secure mobile communication scenario. Specifically, we consider the effect

of Doppler shifts in the channel model and study the joint UAV trajectory and IRS beamforming design to provide safer services to the mobile user.

2) Then, we decompose the original joint design problem into two subproblems and propose the successive convex approximation and phase alignment methods to solve the subproblems. In each iteration, the closed-form expressions for the beamforming matrix and 3D trajectory are derived.

3) For the secure mobile communication scenario, the proposed aerial IRS-assisted 3D joint design can significantly improve the secrecy rate compared to the conventional terrestrial IRS schemes and 2D trajectory designs in the literature.

Notations: Boldface lowercase and uppercase letters denote vectors and matrices, respectively. For a vector $\mathbf{x}$, $\mathbf{x}^H$ and $||\mathbf{x}||$ represent its conjugate transpose and Euclidean norm, respectively. $|x|$ denotes the absolute value of the variable x and $[x]^+ \triangleq \max(x, 0)$.

II. System Model and Problem Formulation

We consider an aerial IRS-assisted secure mobile communication system, which consists of a source B, a legitimate mobile user T, a passive mobile eavesdropper E and a UAV-mounted IRS U. It is assumed that the direct links from the source to the user and the eavesdropper are blocked by obstacles in the urban environment. Thus, the IRS carried by UAV can establish virtual LoS link to the user while guaranteeing the security. Furthermore, assume that the source, the user and the eavesdropper are equipped with a single antenna, while the IRS consists of M reflecting elements. Specifically, we consider a particular UAV's flight time T, which is discretized into N time slots with equal duration $d_t = T/N$, where $\mathcal{N} \triangleq \{1, 2, \cdots, N\}$ denotes the set of slots. Without loss of generality, a 3D Cartesian coordinate system is considered, where the coordinates of the source B and UAV U can be denoted as (x_b, y_b, h_b) and $(x_u[n], y_u[n], h_u[n])$, respectively. Additionally, the coordinates $(x_t[n], y_t[n], 0)$ and $(x_e[n], y_e[n], 0)$ represent the location of the mobile user T and eavesdropper E, respectively.[1] Under the above setting, the mobility constraints of the UAV can be formulated as

$$||\mathbf{q}_u[n] - \mathbf{q}_u[n-1]|| \leq V_{u,h} d_t, \tag{1a}$$

$$|h_u[n] - h_u[n-1]| \leq V_{u,v} d_t, \tag{1b}$$

$$h_{min} \leq h_u[n] \leq h_{max}, \forall n \in \mathcal{N}, \tag{1c}$$

where $\mathbf{q}_u[n] = (x_u[n], y_u[n])$ represents the horizontal coordinate in time slot n. The $V_{u,h}$ and $V_{u,v}$ represent the maximum horizontal and vertical speed of the UAV U, respectively. The symbols h_{min} and h_{max} denote the minimum and maximum flight altitudes of the UAV U, respectively.

Due to the mobility of the UAV, user and eavesdropper, a IRS-ground channel is different from the previous works [8]–[13] and the Doppler shift characterization needs to be considered. Accordingly, the channel coefficients of the B-U-T link and B-U-E link can be defined respectively as

$$h_{BUT}[n] = \boldsymbol{h}_{UT}^H[n] \boldsymbol{\Phi}[n] \boldsymbol{h}_{BU}[n] = \frac{\beta_0}{d_{UT}[n] d_{BU}[n]} \times \sum_{m=1}^{M} e^{j(\theta_m[n] + \frac{2\pi}{\lambda} d(m-1)(\phi_T[n] - \phi_B[n]) + 2\pi n f_{DT})}, \tag{2a}$$

$$h_{BUE}[n] = \boldsymbol{h}_{UE}^H[n] \boldsymbol{\Phi}[n] \boldsymbol{h}_{BU}[n] = \frac{\beta_0}{d_{UE}[n] d_{BU}[n]} \times \sum_{m=1}^{M} e^{j(\theta_m[n] + \frac{2\pi}{\lambda} d(m-1)(\phi_E[n] - \phi_B[n]) + 2\pi n f_{DE})}, \tag{2b}$$

where $d_{ij}[n] = \sqrt{||\mathbf{q}_i[n] - \mathbf{q}_j[n]||^2 + |h_i[n] - h_j[n]|^2}$, $i, j \in \{B, U, T, E\}$, indicates the distance from i to j, and $\boldsymbol{\Phi}[n] = \text{diag}(e^{j\theta_1[n]}, ..., e^{j\theta_M[n]})$, $\theta_m[n] \in [0, 2\pi]$, is the phase-shift matrix of the IRS. The symbols β_0, λ and d denote the reference power gain, carrier wavelength and antenna separation, respectively. In addition, f_{DT} and f_{DE} represent the Doppler terms and can be derived respectively as

$$f_{DT} = \frac{V_t}{\lambda} \phi_T[n] + \frac{V_u}{\lambda} \phi_B[n], \tag{3a}$$

$$f_{DE} = \frac{V_e}{\lambda} \phi_E[n] + \frac{V_u}{\lambda} \phi_B[n], \tag{3b}$$

where V_t, V_e and V_u denote the moving speeds of the user, eavesdropper and UAV, respectively. The symbols $\phi_B[n] = \frac{x_u[n] - x_b}{d_{BU}[n]}$, $\phi_T[n] = \frac{x_u[n] - x_t[n]}{d_{UT}[n]}$ and $\phi_E[n] = \frac{x_u[n] - x_e[n]}{d_{UE}[n]}$ represent the cosine of the angle of arrival and departure of the signal from B to U, U to T, and U to E, respectively.

Based on the above setting, at time slot $n \in \mathcal{N}$, the achievable rate of the legitimate link and the eavesdropping link can be expressed respectively as

$$R_T[n] = \log_2\left(1 + \frac{P[n]|h_{BUT}[n]|^2}{\sigma_t^2}\right), \tag{4a}$$

$$R_E[n] = \log_2\left(1 + \frac{P[n]|h_{BUE}[n]|^2}{\sigma_e^2}\right), \tag{4b}$$

where $P[n]$ denotes the transmit power of the source, and σ_t^2 and σ_e^2 represent the variance of the additive white Gaussian noise at the mobile user and eavesdropper, respectively.

The objective of the problem formulation is to maximize the average secrecy rate $\overline{R}$ over all time slots by jointly designing the UAV 3D trajectory, $\{\mathbf{q}_u[n], h_u[n]\}$, and the IRS phase shift matrix, $\boldsymbol{\Phi}[n]$, subject to the UAV's mobility and IRS's phase shifts constraints. This joint design can be formulated as

$$\begin{aligned} \max_{\{\mathbf{q}_u[n], h_u[n]\}, \boldsymbol{\Phi}[n]} \quad & \frac{1}{N} \sum_{n=1}^{N} \Big[R_T[n] - R_E[n]\Big]^+ \\ \text{s.t.} \quad & (1a) \sim (1c), \\ & 0 \leq \theta_m[n] \leq 2\pi, \forall m, n, \end{aligned} \tag{5}$$

where $[x]^+ \triangleq \max(x, 0)$. Since the secrecy rate $R_T[n] - R_E[n]$ can be always guaranteed to be non-negative by adjusting the transmit power [5], [6], [13], $[\cdot]^+$ will be omitted in the rest of the paper.

[1]Herein, we assume that the user and the eavesdropper follow a set of predefined routes and the aerial IRS can obtain their locations [8]–[12], which is typical for public transports where all vehicles routes can be obtained from the schedule information.

It can be observed that problem (5) is non-convex because the optimization variables $\{\mathbf{q}_{\rm u}[n], h_u[n]\}$ and $\mathbf{\Phi}[n]$ are highly coupled in the objective function. To deal with this challenge, we decompose the original problem into two sub-problems, and solve them iteratively in the next section.

III. Proposed Iterative Algorithm

In this section, the alternating optimization is adopted to obtain an approximated solution to (5) by alternately optimizing one variable while fixing the other one.

A. Optimization of the IRS beamforming matrix $\mathbf{\Phi}[n]$

For a given UAV 3D trajectory $\{\mathbf{q}_{\rm u}[n], h_u[n]\}$, it is obvious that the optimization of the phase shift matrix $\mathbf{\Phi}[n]$ is to maximize the user rate $R_T[n]$. Thus, to maximize the the objective function in (5), we only have to maximize the channel coefficient $h_{BUT}[n]$ in (2a), which can be equivalently rewritten as:

$$h_{BUT}[n]=\frac{\beta_0\sum_{m=1}^{M}e^{j(\theta_m[n]+\Gamma_{UT_m}[n]+\Gamma_{BU_m}[n]+2\pi n f_{DT})}}{d_{UT}[n]d_{BU}[n]}, \quad (6)$$

where $\Gamma_{UT_m}[n] = \frac{2\pi}{\lambda}d(m-1)\phi_T[n]$ and $\Gamma_{BU_m}[n] = -\frac{2\pi}{\lambda}d(m-1)\phi_B[n]$. To maximize the coefficient $h_{BUT}[n]$ in (6), we can align the phases of the received signal at the user. Thus, we set

$$\begin{aligned}&\theta_1[n]+\Gamma_{UT_1}[n]+\Gamma_{BU_1}[n]+2\pi n f_{DT}\\ =&\theta_2[n]+\Gamma_{UT_2}[n]+\Gamma_{BU_2}[n]+2\pi n f_{DT}\\ &\vdots\\ =&\theta_M[n]+\Gamma_{UT_M}[n]+\Gamma_{BU_M}[n]+2\pi n f_{DT}\\ =&\omega,\end{aligned} \quad (7)$$

where ω denotes an arbitrary phase shift with $\omega \in [0, 2\pi]$. Therefore, the optimal phase shifter for the m-th element in the n-th time slot can be derived as

$$\theta_m^*[n] = \omega - \Gamma_{UT_m}[n] - \Gamma_{BU_m}[n] - 2\pi n f_{DT}, \forall n, m. \quad (8)$$

B. Optimization of the UAV 3D trajectory $\{\mathbf{q}_u[n], h_u[n]\}$

For given optimal phase shifts $\theta_m^*[n]$ in (8), the achievable rates for the user and eavesdropper are respectively expressed as

$$R_T^*[n] = \log_2\left(1+\frac{P[n]}{\sigma_t^2}\frac{A^2}{d_{UT}^2[n]d_{BU}^2[n]}\right), \quad (9)$$

$$R_E^*[n] = \log_2\left(1+\frac{P[n]}{\sigma_e^2}\frac{B^2}{d_{UE}^2[n]d_{BU}^2[n]}\right), \quad (10)$$

where $A = \beta_0 M|e^{j\omega}|$ and $B = \beta_0|\sum_{m=1}^{M}e^{j(\frac{2\pi}{\lambda}d(m-1)(\phi_E[n]-\phi_B[n])+2\pi n f_{DE}+\theta_m^*[n])}|$. Thus, problem (5) is simplified as

$$\begin{aligned}\max_{\{\mathbf{q}_{\rm u}[n],h_u[n]\}}\ &\frac{1}{N}\sum_{n=1}^{N}\left(R_T^*[n]-R_E^*[n]\right)\\ \text{s.t. }&(1a)\sim(1c).\end{aligned} \quad (11)$$

Problem (11) is challenging to directly solve due to the UAV trajectory $\{\mathbf{q}_{\rm u}[n], h_u[n]\}$ constraints in the numerator and denominator of $R_E^*[n]$. Hence, we first define an upper bound on $R_E^*[n]$ as follows:

$$\begin{aligned}R_E^*[n] &= \log_2\left(1+\frac{P[n]}{\sigma_e^2}\frac{B^2}{d_{UE}^2[n]d_{BU}^2[n]}\right)\\ &\le \log_2\left(1+\frac{P[n]}{\sigma_e^2}\frac{A^2}{d_{UE}^2[n]d_{BU}^2[n]}\right).\end{aligned} \quad (12)$$

Then, by introducing a set of slack variables $u[n]$, $v[n]$, $r[n]$ and $k_i[n]$, $i \in \{1, 2\}$, the problem defined in (11) reduces to the following problem:

$$\begin{aligned}\max_{\{\mathbf{q}_{\rm u}[n],h_u[n]\},u[n],v[n],r[n],k_i[n]}\ &\frac{1}{N}\sum_{n=1}^{N}\left[\log_2\left(1+\frac{P[n]A^2}{\sigma_t^2u[n]v[n]}\right)-r[n]\right]\\ \text{s.t. }&C1: u[n] \ge ||\mathbf{q}_u[n]-\mathbf{q}_t[n]||^2+|h_u[n]|^2,\\ &C2: v[n] \ge ||\mathbf{q}_u[n]-\mathbf{q}_b||^2+|h_u[n]-h_b|^2,\\ &C3: r[n] \ge \log_2\left(1+\frac{P[n]A^2}{\sigma_e^2}e^{k_1[n]+k_2[n]}\right),\\ &C4: e^{-k_1[n]} \le ||\mathbf{q}_u[n]-\mathbf{q}_e[n]||^2+|h_u[n]|^2,\\ &C5: e^{-k_2[n]} \le ||\mathbf{q}_u[n]-\mathbf{q}_b||^2+|h_u[n]-h_b|^2,\\ &(1a)\sim(1c).\end{aligned} \quad (13)$$

To efficiently solve problem (13), we introduce an important lemma as follows.

LEMMA 1. *Function* $\log_2\left(1+\frac{P[n]A^2}{\sigma_t^2u[n]v[n]}\right)$ *is convex with respect to* $u[n]$ *and* $v[n]$.

Proof: Please refer to Appendix A. ■

Based on Lemma 1, we apply the first-order Taylor series expansions of $\log_2\left(1+\frac{P[n]A^2}{\sigma_t^2u[n]v[n]}\right)$ as follows:

$$\begin{aligned}\log_2\left(1+\frac{P[n]A^2}{\sigma_t^2u[n]v[n]}\right)\ge&\log_2 t_1^l[n]+\frac{t_2^l[n]}{\ln 2 t_1^l[n]}(u[n]-u_l[n])\\ &+\frac{t_3^l[n]}{\ln 2 t_1^l[n]}(v[n]-v_l[n]),\end{aligned} \quad (14)$$

where $t_1^l[n] = 1+\frac{P[n]}{\sigma_t^2}\frac{A^2}{u_l[n]v_l[n]}$, $t_2^l[n] = -\frac{P[n]}{\sigma_t^2}\frac{A^2}{u_l^2[n]v_l[n]}$ and $t_3^l[n] = -\frac{P[n]}{\sigma_t^2}\frac{A^2}{u_l[n]v_l^2[n]}$, and $u_l[n]$ and $v_l[n]$ are the feasible solutions obtained at the l-th iteration. Similarly, the constraints C4 and C5 in (13) can be equivalently rewritten as follows:

$$\begin{aligned}e^{-k_1[n]} \le&||\mathbf{q}_u^l[n]-\mathbf{q}_e[n]||^2+|h_u^l[n]|^2\\ &+2(\mathbf{q}_u^l[n]-\mathbf{q}_e[n])^T(\mathbf{q}_u[n]-\mathbf{q}_u^l[n])\\ &+2(h_u^l[n])^T(h_u[n]-h_u^l[n]),\end{aligned} \quad (15)$$

$$\begin{aligned}e^{-k_2[n]} \le&||\mathbf{q}_u^l[n]-\mathbf{q}_b||^2+|h_u^l[n]-h_b|^2\\ &+2(\mathbf{q}_u^l[n]-\mathbf{q}_b)^T(\mathbf{q}_u[n]-\mathbf{q}_u^l[n])\\ &+2(h_u^l[n]-h_b)^T(h_u[n]-h_u^l[n]),\end{aligned} \quad (16)$$

Algorithm 1 The Proposed Iterative Algorithm

Initialize $\{\mathbf{q}_u^0[n], h_u^0[n]\}$, $\mathbf{\Phi}^0[n]$ and $\overline{R}^0$.
Set the tolerance ϵ and the iteration number $l = 1$.
Repeat
Calculate $\{\mathbf{q}_u^l[n], h_u^l[n]\}$ of (17) for given $\mathbf{\Phi}^{(l-1)}[n]$.
Update $\mathbf{\Phi}^l[n]$ by using (8) under given $\{\mathbf{q}_u^l[n], h_u^l[n]\}$.
Determine $\overline{R}^l = \frac{1}{N}\sum_{n=1}^{N}(R_T[n] - R_E[n])$ based on (5).
Let $l = l + 1$.
Until $|\overline{R}^l - \overline{R}^{(l-1)}| < \epsilon$.
Output: $\{\mathbf{q}_u^l[n], h_u^l[n]\}$, $\mathbf{\Phi}^l[n]$ and $\overline{R}^l$.

where $\mathbf{q}_u^l[n]$ and $h_u^l[n]$ are the feasible solutions obtained at the l-th iteration.

As a result, by substituting (14)−(16) into (13), we rewrite the problem in (13) into an equivalent form as

$$\begin{aligned}\max_{\{\mathbf{q}_u[n],h_u[n]\},u[n],v[n],r[n],k_l[n]} \; & \frac{1}{N}\sum_{n=1}^{N}\Big[\log_2 t_1^l[n] + \frac{t_2^l[n]}{\ln 2 t_1^l[n]}(u[n] \\ & - u_l[n]) + \frac{t_3^l[n]}{\ln 2 t_1^l[n]}(v[n] - v_l[n]) - r[n]\Big] \\ \text{s.t. } & C1 \sim C3, \\ & (15), (16), (1).\end{aligned} \tag{17}$$

Note that problem (17) is a convex optimization problem, which can be optimally solved by existing standard optimization solvers such as CVX.

C. Overall algorithm

In this subsection, we combine the proposed solution approaches in subsections A and B to develop an iterative algorithm, which is summarized in Algorithm 1. In each iteration, the IRS beamforming matrix $\mathbf{\Phi}[n]$ and the UAV 3D trajectory $\{\mathbf{q}_u[n], h_u[n]\}$ are alternately solved by using the existing standard optimization techniques, and thus a suboptimal solution of problem (5) can be obtained by the proposed iterative algorithm; the relevant details can be found in [5], [6]. Besides, the complexity of the proposed iterative algorithm is $\mathcal{O}[N_{ite}(N)^{3.5}]$, where N_{ite} and N denote the numbers of required iterations and time slots, respectively.

IV. Simulation results

The simulation parameters are set as follow. The coordinates of the initial and final positions of UAV U are set to $(x_u[0], y_u[0], h_u[0]) = (0, 100, 60)$ m and $(x_u[N], y_u[N], h_u[N]) = (600, 100, 60)$ m, respectively. The source B coordinate is $(x_b, y_b, h_b) = (0, 0, 10)$ m. Furthermore, unless otherwise specified, we set $N = 40$, $M = 128$, $V_{u,h} = 20$ m/s, $V_{u,v} = 20/\sqrt{2}$ m/s [5], [6], [8], $h_{min} = 20$ m, $h_{max} = 60$ m, $V_t = 11.5$ m/s, $V_e = 7.5$ m/s, $\beta_0 = -20$ dB, $d = \lambda/2$, $P[n] = 10$ dBm and $\sigma_t^2 = \sigma_e^2 = -80$ dBm [9], [10], [13], respectively.

Fig. 1(a) depicts the trajectories of the UAV onto the 3D plane with different maximum horizontal speeds $V_{u,h}$. The symbols $\times$ denote the position of the source, while $\triangle$ and $\bigtriangledown$ represent the initial and final positions of the UAV, user and eavesdropper, respectively. As shown in Fig. 1(a), when $V_{u,h}$ is small, i.e., $V_{u,h} = 15$ m/s, the UAV U almost directly flies to the final position and climbs the flight height for a certain period of time. The reason is that there is a minimum flight time N constraint while the UAV U needs to steer away from the location of the mobile eavesdropper E to enhance the secrecy rate. Fig. 1(b) plots the 3D trajectories of the UAV versus different numbers of reflection elements M. From Fig. 1(b), the UAV U moves closer to the source and climbs the flight height to keep away from the eavesdropper as M decreases. Moreover, the achievable average secrecy rate of the proposed joint design increases as M increases. This is because when M is sufficiently large, the aerial IRS does not need to move closer to the user to reflect information, which results in less information intercepted by the E. Fig. 1(c) illustrates the achievable secrecy rate versus different eavesdropper speeds V_e. As can be seen in Fig. 1(c), the achieved secrecy rate first decreases and then increases as N increases for all considered values of V_e. This is because the eavesdropper E first approaches to the user T, and gradually keeps away from it as N increases. Moreover, it is worth noting that when $V_e = 3.75$ m/s, the achieved secrecy rate first become saturated and then decreases rapidly in the latter half of flight time N. This is because when V_e is small, the aerial IRS U is far from the eavesdropper E as N increases, and finally flies to the final location due to the flight time limitation.

Fig. 2 compares the performance of our proposed aerial IRS-assisted 3D joint design (denoted as Proposed scheme) with two benchmark schemes, namely: 1) The 2D joint design scheme (denoted as 2D scheme), i.e., the UAV U flight altitude $h_u[n] = 30$ m; 2) The fixed IRS design scheme (FIRS scheme), i.e., the IRS on the fixed location $(x_u, y_u, h_u) = (200, 100, 20)$ m. Fig. 2 shows an expected observation that the Proposed scheme achieves a superior performance compared to that of the 2D and FIRS schemes. In addition, it is worth noting that the achieved secrecy rate of the FIRS scheme remains constant for different N values. This implies that a fixed IRS will not provide a high-level security performance to the mobile communication scenario.

V. Conclusion

This paper proposed a novel aerial IRS-assisted secure mobile communication system. In the considered scheme, the 3D trajectory of the UAV and the phase-shift matrix of the IRS were optimized jointly to maximize the average secrecy rate under the UAV's mobility and IRS's phase shifts constraints. Different from the most previous works which use the free space path loss model to simplify the analysis, we considered the effect of Doppler shifts in the channel model. Simulation results confirmed that for the secure mobile scenario, adopting

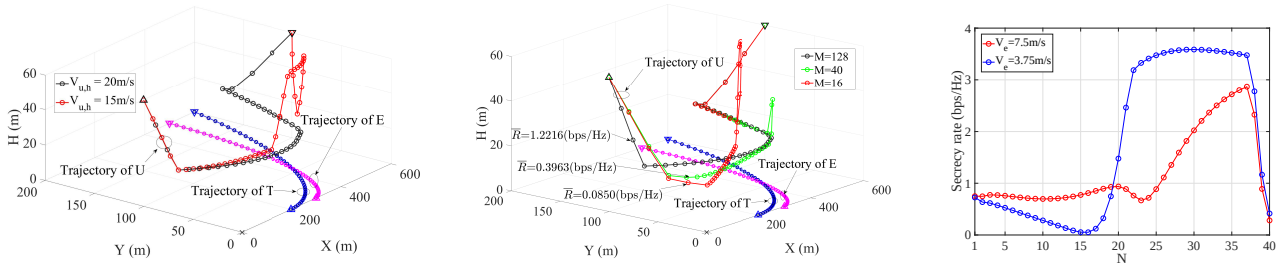

(a) (b) (c)

Fig. 1: (a) Optimized UAV trajectories with different speeds $V_{u,h}$; (b) Optimized UAV trajectories with different M; (c) Achieved secrecy rates at different speed V_e.

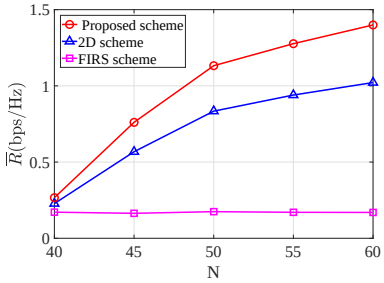

Fig. 2: Achieved average secrecy rates of different algorithms.

the proposed aerial IRS-assisted 3D joint design can achieve a significant improvement in the secrecy rate compared to the reference schemes.

Appendix A
Proof of Lemma 1

Let $f(u[n], v[n])$ denote the first term in the objective function of (13). Then, we obtain the second-order partial derivative of $f(u[n], v[n])$ with respect to $u[n]$ and $v[n]$, respectively, as:

$$\frac{\partial^2 f}{\partial u^2[n]} = \frac{\frac{2P[n]A^2}{\sigma_t^2} v^{-1}[n]u^{-3}[n] + (\frac{P[n]A^2}{\sigma_t^2})^2 v^{-2}[n]u^{-4}[n]}{\ln 2(1+\frac{P[n]A^2}{\sigma_t^2}u^{-1}[n]v^{-1}[n])^2}, \quad (18)$$

$$\frac{\partial^2 f}{\partial v^2[n]} = \frac{\frac{2P[n]A^2}{\sigma_t^2} u^{-1}[n]v^{-3}[n] + (\frac{P[n]A^2}{\sigma_t^2})^2 u^{-2}[n]v^{-4}[n]}{\ln 2(1+\frac{P[n]A^2}{\sigma_t^2}u^{-1}[n]v^{-1}[n])^2}, \quad (19)$$

$$\frac{\partial^2 f}{\partial u[n]\partial v[n]} = \frac{\frac{P[n]A^2}{\sigma_t^2} u^{-2}[n]v^{-2}[n]}{\ln 2(1+\frac{P[n]A^2}{\sigma_t^2}u^{-1}[n]v^{-1}[n])^2}, \quad (20)$$

$$\frac{\partial^2 f}{\partial v[n]\partial u[n]} = \frac{\frac{P[n]A^2}{\sigma_t^2} v^{-2}[n]u^{-2}[n]}{\ln 2(1+\frac{P[n]A^2}{\sigma_t^2}u^{-1}[n]v^{-1}[n])^2}. \quad (21)$$

Thus, the Hessian of $f(u[n], v[n])$ can be expressed as:

$$\nabla^2 f = \begin{bmatrix} \frac{\partial^2 f}{\partial u^2[n]} & \frac{\partial^2 f}{\partial u[n]\partial v[n]} \\ \frac{\partial^2 f}{\partial v[n]\partial u[n]} & \frac{\partial^2 f}{\partial v^2[n]} \end{bmatrix}. \quad (22)$$

Based on $f(u[n], v[n])$ defined in (13) and due to the fact that $\{u[n], v[n], P[n], \sigma_t^2, A\} > 0$, we have $\frac{\partial^2 f}{\partial u^2[n]} > 0$ and $\frac{\partial^2 f}{\partial u^2[n]}\frac{\partial^2 f}{\partial v^2[n]} - \frac{\partial^2 f}{\partial u[n]\partial v[n]}\frac{\partial^2 f}{\partial v[n]\partial u[n]} > 0$, which shows that the matrix $\nabla^2 f$ is positive definite. Hence, $f(u[n], v[n])$ is a convex function. This completes the proof.

References

[1] Y. Zeng, R. Zhang, and J. Teng, "Wireless communications with unmanned aerial vehicles: Opportunities and challenges," *IEEE Commun. Mag.*, vol. 54, no. 5, pp. 36-42, Oct. 2016.

[2] L. Gupta, R. Jain, and G. Vaszkun, "Survey of important issues in UAV communication networks," *IEEE Commun. Surveys Tuts.*, vol. 18, no. 2, pp. 1123-1152, Second quarter 2016.

[3] X. Sun, D. W. K. Ng, Z. Ding, Y. Xu, and Z. Zhong, "Physical layer security in UAV systems: Challenges and opportunities," *IEEE Wireless Commun.*, vol. 26, no. 5, pp. 40-47, Oct. 2019.

[4] Q. Wu, W. Mei, and R. Zhang, "Safeguarding wireless network with UAVs: A physical layer security perspective," *IEEE Wireless Commun.*, vol. 26, no. 5, pp. 12-18, Oct. 2019.

[5] W. Wang et al., "Energy-constrained UAV-assisted secure communications with position optimization and cooperative jamming," *IEEE Trans. Commun.*, vol. 68, no. 7, pp. 4476-4489, Jul. 2020.

[6] W. Wang et al., "Robust 3D-trajectory and time switching optimization for dual-UAV-enabled secure communications," *IEEE J. Sel. Areas Commun.*, vol. 39, no. 11, pp. 3334-3347, Nov. 2021.

[7] C. You, Z. Kang, Y. Zeng, and R. Zhang, "Enabling smart reflection in integrated air-ground wireless network: IRS meets UAV," *IEEE Wireless Commun.*, vol. 28, no. 6, pp. 138-144, Dec. 2021.

[8] S. Fang, G. Chen, and Y. Li, "Joint optimization for secure intelligent reflecting surface assisted UAV networks," *IEEE Wireless Commun. Lett.*, vol. 10, no. 2, pp. 276-280, Feb. 2021.

[9] S. Li, B. Duo, M. D. Renzo, M. Tao, and X. Yuan, "Robust secure UAV communications with the aid of reconfigurable intelligent surfaces," *IEEE Trans. Wireless Commun.*, vol. 20, no. 10, pp. 6402-6417, Oct. 2021.

[10] X. Pang, N. Zhao, J. Tang, C. Wu, D. Niyato, and K. K. Wong, "IRS-assisted secure UAV transmission via joint trajectory and beamforming design," *IEEE Trans. Commun.*, vol. 70, no. 2, pp. 1140-1152, Feb. 2022.

[11] X. Guo, Y. Chen, and Y. Wang, "Learning-based robust and secure transmission for reconfigurable intelligent surface aided millimeter wave UAV communications," *IEEE Wireless Commun. Lett.*, vol. 10, no. 8, pp. 1795-1799, Aug. 2021.

[12] H. Niu, Z. Chu, Z. Zhu, and F. Zhou, "Aerial intelligent reflecting surface for secure wireless networks: Secrecy capacity and optimal trajectory strategy," *Intell. Converged Netw.*, vol. 3, no. 1, pp. 119-133, Mar. 2022.

[13] W. Wei, X. Pang, J. Tang, N. Zhao, X. Wang, and A. Nallanathan, "Secure transmission design for aerial IRS assisted wireless networks," *IEEE Trans. Commun.*, vol. 71, no. 6, pp. 3528-3540, Jun. 2023.